Final Draft

of the original manuscript

Scheuerlein, C.; Gan, W.; Hofmann, M.; Katzer, B.:
Texture in Superconducting Magnet Constituent Materials and Its Effect on Elastic Anisotropy.
In: IEEE Transactions on Applied Superconductivity. Vol. 29 (2019) 5, 7800105.

First published online by IEEE: 30.01.2019

https://dx.doi.org/10.1109/TASC.2019.2896452

….

Texture in superconducting magnet constituent materials and its effect on elastic anisotropy

Christian Scheuerlein, Weimin Gan, Michael Hofmann, and Balduin Katzer

***Abstract*— The materials used in superconducting magnet coils and in the structural magnet constituents are textured to various extents. This causes an angular dependence of the Young's moduli that needs to be taken into account when predicting the stress and strain distribution in the magnets. We have measured by neutron diffraction the texture in metallic materials typically used in superconducting magnets. Based on the neutron diffraction data the elastic anisotropy of the different materials has been calculated. Among the materials studied, the extruded Al oxide dispersion strengthened Cu coil wedges exhibit the strongest elastic anisotropy of 37%. The Young's moduli calculated from single crystal elastic constants and grain orientation distributions are compared with highly accurate Young's moduli derived experimentally from resonance tests.**

***Index Terms*—Superconducting magnet, Nb_3Sn, Cu, DISCUP, stainless steel, Al 7175, anisotropy, Young's modulus, neutron diffraction**

I. INTRODUCTION

THE LHC High Luminosity upgrade (HL-LHC) [1] requires the installation of new superconducting magnets [2] based on Nb_3Sn technology. Very high field Nb_3Sn magnets are also studied for the Future Circular Collider (FCC) project [3].

To control the stress distribution in superconducting magnet components under the huge Lorentz forces is a main challenge in the magnet design. Most of the magnet and conductor constituent materials are textured, and exhibit anisotropic materials properties. The mechanical anisotropy needs to be taken into account when predicting the stress and strain distribution in the magnets at the different assembly and operation stages.

The stress-strain behavior is usually determined from uniaxial stress-strain measurements [4],[5]. The goal of the present study is to determine how the Young's modulus of the different magnets materials depends on the load direction.

Previously we have studied the texturing of the fine-grained Nb_3Sn filaments and its effect on the elastic properties by Electron Backscatter Diffraction (EBSD) [6]. For other more coarse grained materials like the annealed Cu stabiliser EBSD could not provide the necessary texture information.

Neutron diffraction is commonly used for obtaining a global texture description that enables the determination of the angular dependence of the Young's modulus. We have measured by neutron diffraction the texture in metallic materials typically used in superconducting magnets. Based on the neutron diffraction data the elastic anisotropy of the different magnet and composite superconductor constituents has been calculated.

The Magnetil, YUS-130, DISCUP and Nb_3Sn/Cu conductor block samples were extracted from 11 T dipole prototype components [7],[8]. Uniaxial static stress-strain and dynamic mechanical test results for these materials are presented in [4]. The Al 7175 sample was extracted from a MQXF prototype magnet shell [9].

II. TEXTURE MEASUREMENTS AT STRESS-SPEC

Neutron texture measurements have been performed at the STRESS-SPEC instrument at MLZ [10], with a wavelength of about 1.683 Å produced from a Ge(311) single-crystal monochromator. The incoming beam size was Ø25 mm while the diffracted beam side was open. Pole figures were measured with the STRESS-SPEC robotic system using a continuous scanning routine [11] (Fig. 1).

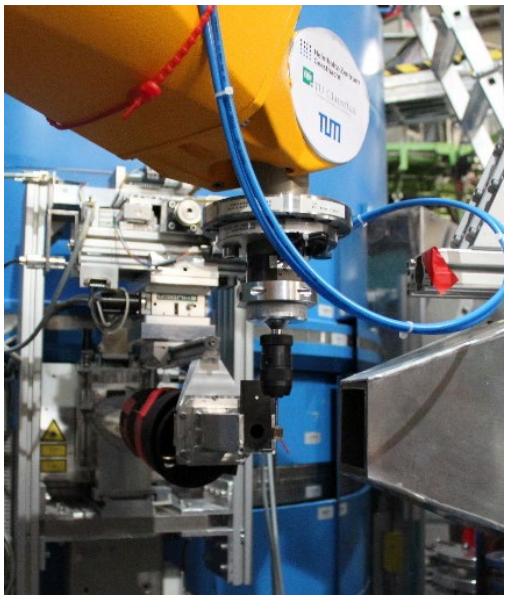

Fig 1: Set-up for texture measurements using a robotic system.

III. CALCULATION OF ANGULAR DEPENDENCE OF THE YOUNG'S MODULI FROM SINGLE CRYSTAL ELASTIC CONSTANTS

The orientation distribution functions (ODFs) were calculated using the measured complete pole figures using the harmonic series expansion method. With the calculated C-coefficient and the single crystal elastic constants (SEC) [12], the triaxial bulk Young's moduli were calculated for the different samples using the Cub_PHY program based on a cluster model [13],[14].

C. Scheuerlein and B. Katzer are with CERN, CH-1211 Geneva 23, Switzerland, (corresponding author phone: ++41 (0)22 767 8022, E-mail: Christian.Scheuerlein@cern.ch).

W. Gan is with German Engineering Materials Science Centre at MLZ, Helmholtz-Zentrum Geesthacht, Germany.

M. Hofmann is with Forschungsneutronenquelle Heinz Maier-Leibnitz (FRM II), TU München, Germany

….

Effective Young's moduli of polycrystalline materials can be calculated with the assumptions that either the strain (Voigt [15]) or the stress (Reuss [16]) are constant in the entire material. In most cases, the experimentally determined Young's moduli lie between the upper and lower bounds predicted by these models. For many materials, the experimentally determined Young's moduli are close to those calculated according to the Hill model [17], which is the arithmetic mean of the Reuss and Voigt values, taking into account the effect of grain interactions [14].

IV. Results

A Low carbon steel yoke (Magnetil)

The 11 T dipole yoke is made of hot rolled sheets of an ultralow carbon steel with C content of less than 0.0025% (trademark "Magnetil"). The texturing produced by the rolling process improves the magnetic properties of the yoke [18]. For texture measurements two 5.8 mm-thick samples with 10×10 mm^2 cross section extracted from a Magnetil yoke sheet have been used. The Fe (110) pole figure presented in Fig. 2 reveals a {110} and {100} texture in <110> direction, which is due to the sheet rolling at 800 °C [18].

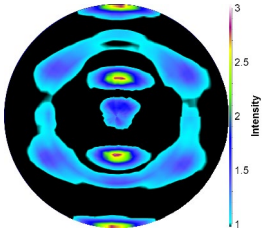

Fig 2: Fe (110) pole figure of the Magnetil sheet.

The calculated angular dependence of the Magnetil Young's modulus is presented in Fig. 3. The Young's moduli determined experimentally by resonance measurements are $E_{Magnetil\_L}$=196 GPa and $E_{Magnetil\_T}$=219 GPa [4].

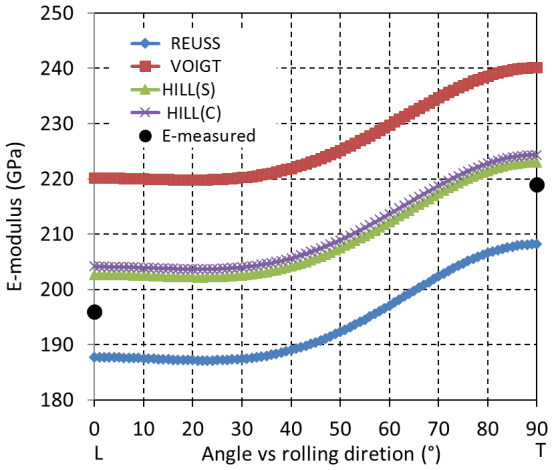

Fig. 3: Magnetil Young's modulus as a function of the angle with respect to the rolling direction L (at 0°), whereby T is the transverse direction. The circular symbols indicate the experimentally determined Young's moduli in L and T directions [4].

B Austenitic stainless steel collar (YUS-130)

The 3 mm-thick collars of the 11 T dipole magnets are made by fine-blanking of austenitic steel X8CrMnNiN19-11-6 sheet, which is also known under the tradename YUS-130 [19]. Samples for texture measurements were cut from the nose of the 11 T dipole collars. The L (rolling) direction is in the direction of the nose pressing onto the pole wedge. The YUS-130 pole figures are shown in Fig. 4.

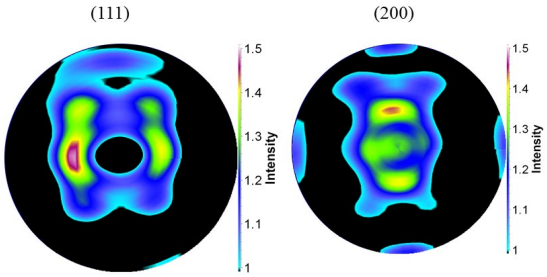

Fig 4: Austenite (111) and (200) pole figures of the YUS-130 sheet.

The Young's modulus dependence on the angle with respect to the rolling direction is presented in Fig. 5. From resonance measurements the Young's moduli $E_{YUS\text{-}130\_L}$=196 GPa, and $E_{YUS\text{-}130\_T}$=192 GPa were determined [4].

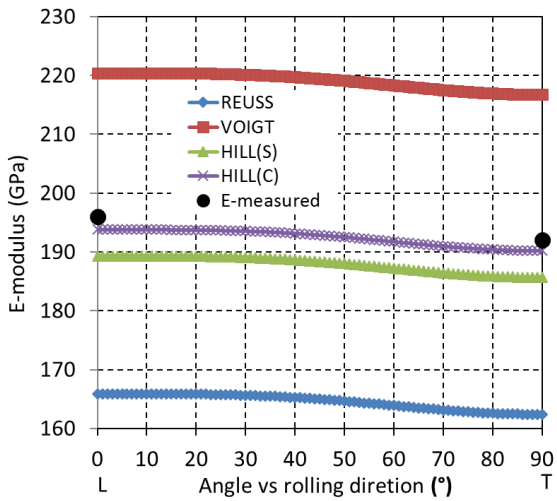

Fig. 5: YUS-130 Young's modulus as a function of the angle with respect to the rolling direction L (at 0°), whereby T is the transverse direction. The circular symbols indicate the experimentally determined Young's moduli in L and T directions [4].

C Dispersion strengthened Cu coil wedge (DISCUP)

The 11 T dipole coil wedges between the conductor blocks are made of aluminum oxide dispersion strengthened copper with the tradename "CEP DISCUP® C3/30". This contains 0.6 wt.% Al, and has an ultra-fine structure with a texture in the direction of extrusion [20],[4]. The Cu pole figures of the DISCUP sample of Fig. 6 shows a main α <110> fiber with a weak cube {001}<100> component and a weak Goss {110}<001> component, as expected for hot extruded fcc metals.

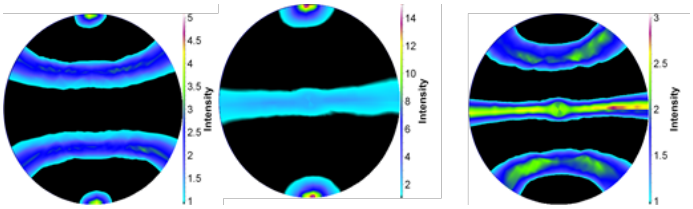

Fig 6: Cu (111), Cu (200) and Cu (220) pole figures of DISCUP.

The angular dependence of the DISCUP Young's modulus calculated from the ODF is presented in Fig. 7. For

comparison, the Young's moduli determined by compression stress-strain measurements in the extrusion direction (89 GPa) and perpendicular to the extrusion direction (96 GPa) are shown as well [4].

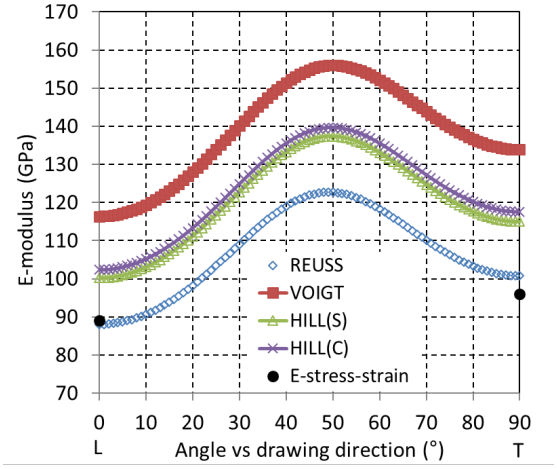

Fig 7: DISCUP Young's modulus as a function of the angle with respect to the wedge extrusion direction L (at 0°). The circular symbols indicate the experimentally determined Young's moduli in L and T directions.

D Nb₃Sn/Cu coil conductor block

The 11 T dipole coils consist of six conductor blocks, which are wound from non-reacted Nb_3Sn keystoned Rutherford type cable. The brittle Nb_3Sn is formed during a reaction heat treatment with a peak temperature of 650 °C. The textured Nb_3Sn filaments exhibit anisotropic materials properties [21].

A 15×15×15 mm³ Nb_3Sn/Cu cube sample extracted from 11 T dipole short model coil #107 has been used for texture measurements. For more information about the Nb_3Sn/Cu sample see reference [22]. The Nb_3Sn (200), Nb_3Sn (211), Cu (111) and Cu (200) pole figures are shown in Fig. 8.

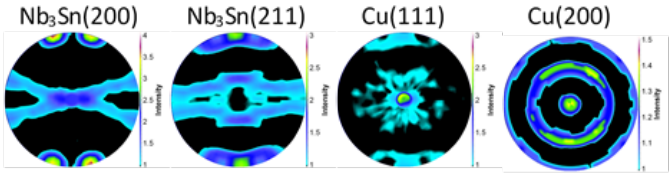

Fig 8: Nb_3Sn (200), Nb_3Sn (211), Cu (111) and Cu (200) pole figures.

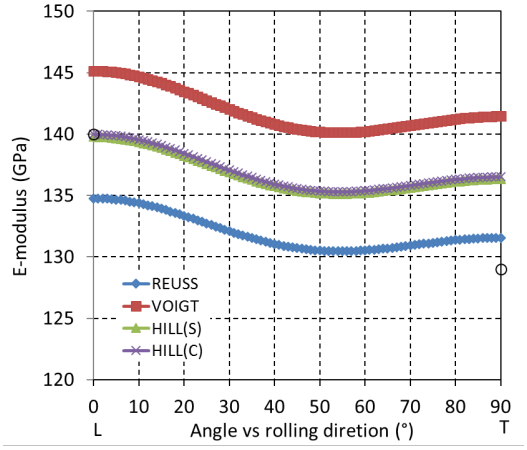

Fig. 9: Nb_3Sn in coil #107 Young's modulus as a function of the angle with respect to the drawing direction A (at 0°). Open circles indicate the Young's moduli determined from SEC and EBSD data of a RRP wire.

The angular dependence of the Nb_3Sn Young's modulus calculated using the Nb_3Sn crystal elastic constants [20] is presented in Fig. 9. For comparison, the Young's moduli of the Nb_3Sn filament in a RRP wire calculated from EBSD data are shown as well (E_{axial}=140 GPa and E_{trans}=129 GPa, respectively [21]). The comparatively smaller elastic anisotropy in the coil samples can be partly explained by the wire transposition pitch in the Rutherford type cables of the coil.

In the reacted RRP type wires Nb_3Sn exhibits a <100> growth texture, with a very small <110> component remanent from the Nb drawing texture [6]. After the coil reaction the Cu stabiliser exhibits a duplex texture with <111> and <200> orientations in the axial direction [23].

The angular dependence of the Cu stabiliser Young's modulus in coil #107 is presented in Fig. 10. The elastic anisotropy in the Cu stabiliser is much smaller than in the extruded DISCUP coil wedges (Fig. 7). In the Cu stabiliser the maximum Young's modulus is in the axial direction, while in the DISCUP coil wedges it is obtained when the load is applied in an angle of 50° with respect to the axial direction.

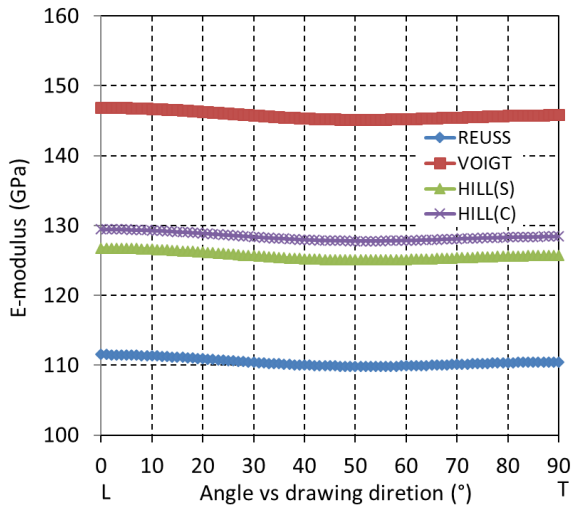

Fig. 10: Annealed Cu Young's modulus in 11 T dipole coil #107 as a function of the angle with respect to the drawing direction.

The Young's moduli of a hard drawn Cu wire before and after full annealing in the wire drawing direction derived from stress-strain measurements are 127 GPa and 108 GPa, respectively [4]. Since the loading stress-strain curves of annealed Cu do not exhibit a pronounced linear part, the annealed Cu Young's modulus value has a relatively large uncertainty in the order of 10% [4].

E Aluminum alloy shrinking cylinder (Al 7175)

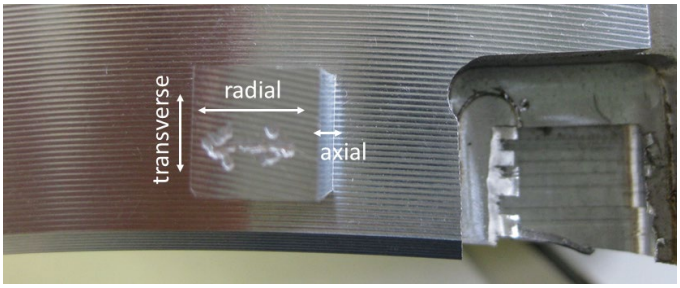

Fig. 11: Aluminum 7175 sample 10×10×10 mm³ cut from Al magnet shell for texture measurements with definition of the principal directions.

….

The Al 7175 alloy (EN AW-7175), temper designation T74 [24] is used for the outer shrinking cylinder of the MQXF quadrupole magnets. Al 7175 is alloyed with about 6% zinc, and less magnesium and copper.

For texture measurements a 10×10×10 mm^3 Al 7175 cube samples was cut out from the 29 mm thick MQXF magnet shell. For the Al 7175 sample the rolling direction "L" corresponds with the radial direction and "T" with the transverse direction, as defined in Fig. 11. The Al (111) and Al (200) pole figures of the Al 7175 alloy are presented in Fig. 12, showing a {211} texture in <111> direction and a {100} texture in <100> direction, as it is commonly observed in rolled aluminium alloys [25].

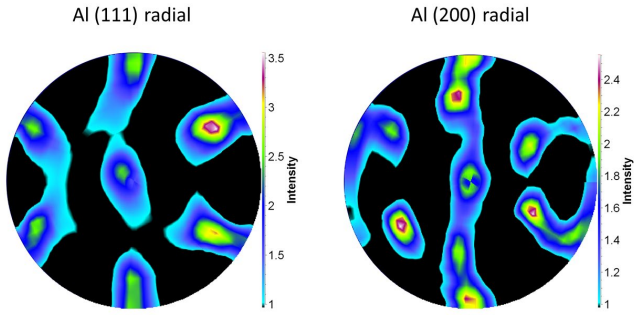

Fig. 12: Al (111) and Al (200) pole figures of Al 7175.

The Al 7175 Young's modulus angular dependence is presented in Fig. 13. Only a very small elastic anisotropy is observed. The Young's modulus in L direction obtained eperimentally with the resonance method is 69.2 GPa [26], which is 1% lower than the value calculated from SEC with the Reuss assumption. This small difference can be explained by the uncertainty of the resonance test, which is about 1% [4].

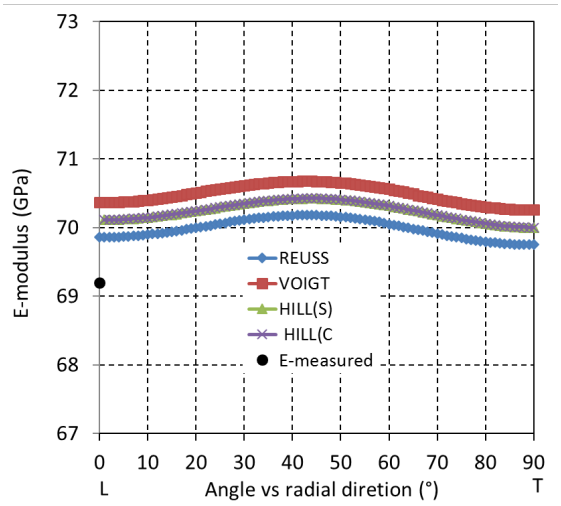

Fig. 13: Al 7175 Young's modulus as a function of the angle with respect to the drawing direction. The circular symbol indicates the experimentally determined Young's modulus in L direction.

V. Discussion and Conclusion

Finite element (FE) models are an essential tool for the design of superconducting high field magnets. The results presented here can be used to further refine FE models, which require as input reliable materials data.

All magnet metals studied here exhibit a strong preferential crystal orientation, and some a pronounced elastic anisotropy. The extent of elastic anisotropy is summarised in Table I, where the relative Young's modulus differences with respect to those calculated in the L direction are compared. The L direction is the wire drawing or wedge extrusion direction, or for sheets the rolling direction.

TABLE I
YOUNG'S MODULUS IN T DIRECTION, MAXIMUM (MAX) AND MINIMUM (MIN) IN PERCENT OF THE MODULUS IN L DIRECTION. THE ANGLES WHERE THE MAX AND MIN VALUES OCCUR ARE CALCULATED WITH RESPECT TO THE L DIRECTION.

Material	E in percent of E in L direction (%)				
	Transverse	max	angle	min	angle
Magnetil	110	110	90°	100	0°
Al 7175	99.8	100.5	43°	99.8	90°
YUS-130	98.1	100	0°	98.1	90°
DISCUP	115	137	50°	100	0°
Cu stabiliser	99.1	100	0°	98.6	53°
Nb_3Sn	97.6	100	0°	96.7	54°

The measured YUS-130 and Magnetil Young's moduli are within the upper and lower bounds calculated according to Reuss and Voigt, and are close to the calculated Hill values. For Al 7175 the measured Young's modulus is 1.0% and 1.6% smaller than the Reuss and Voigt calculations, respectively.

Among the materials studied here, the extruded Al oxide dispersion strengthened Cu (DISCUP C30) wedges exhibit the strongest elastic anisotropy of 37%. The Young's modulus of 89 GPa measured in the L direction corresponds with that calculated assuming iso-stress conditions (Reuss). This value is significantly lower than the modulus of pure Cu. The measured T value of 96 GPa is slightly lower than the one obtained by the Reuss calculation. The calculation relies strongly on the SEC. For the calculation of the DISCUP moduli the SEC of pure Cu were used, which may be a reason for the discrepancy between calculated and measured Young's moduli.

In contrast to DISCUP, the pure annealed Cu stabilizer in the Nb_3Sn conductor exhibits only a small elastic anisotropy that may be neglected in FE calculations.

The direct measurement of Nb_3Sn filament Young's moduli is extremely challenging because samples appropriate for standardized mechanical tests cannot be produced. Therefore, Nb_3Sn elastic anisotropy can only be determined from the grain orientation distribution and SECs. The difference between the L and T Young's moduli calculated from neutron diffraction data (this study) and from previous EBSD data obtained for wires is partly explained by the misalignment of the L and T directions in the coil due to the cable transposition pitch.

Acknowledgements

We are grateful to the CERN central workshop team for the preparation of the test specimen. This work is based upon experiments performed at the STRESS-SPEC instrument operated by FRM II at the Heinz Maier-Leibnitz Zentrum (MLZ), Garching, Germany. This work was supported by the European Commission under the FP7 project HiLumi LHC under Grant GA 284404, co-funded by the DoE, USA and KEK, Japan.

….

REFERENCES

[1] The High Luminosity Large Hadron Collider, ed. O. Bruening and L. Rossi, World Scientific Publishing Co, (2015)

[2] L. Bottura, G. de Rijk, L. Rossi, E. Todesco, "Advanced accelerator magnets for upgrading the LHC," *IEEE Trans. Appl. Supercond*., vol. 22, no. 3, 2012, Art. no. 4002008

[3] D. Tommasini et al., "The 16 T Dipole Development Program for FCC", *IEEE Trans. Appl. Supercond*., vol. 27, no. 4, June 2017, Art. no. 4000405

[4] C. Scheuerlein, F. Lackner, F. Savary, B. Rehmer, M. Finn, P. Uhlemann, "Mechanical properties of the HL-LHC 11 Tesla Nb_3Sn magnet constituent materials", *IEEE Trans. Appl. Supercond*., vol. 27, no. 4, 2017, Art. no. 4003007

[5] C. Scheuerlein, F. Lackner, F. Savary, B. Rehmer, M. Finn, C. Meyer, "Thermomechanical behavior of the HL-LHC 11 Tesla Nb_3Sn magnet coil constituents during reaction heat treatment", *IEEE Trans. Appl. Supercond*., vol. 28, no. 3, 2018, Art. no. 4003806

[6] C. Scheuerlein, G. Arnau, P. Alknes, N. Jimenez, B. Bordini, A. Ballarino, M. Di Michiel, L. Thilly, T. Besara, T. Siegrist, "Nb_3Sn texture in state-of-the-art multifilamentary superconducting wires", *Supercond. Sci. Technol*., vol. 27, 2014, Art. no. 025013

[7] M. Karppinen et al., "Design of 11 T twin-aperture dipole demonstrator magnet for LHC upgrades", *IEEE Trans. App. Supercond*., vol. 22, no. 3, June 2012, Art. no. 4901504

[8] F. Savary et al., "Progress on the Development of the Nb3Sn 11T Dipole for the High Luminosity Upgrade of LHC," *IEEE Trans. Appl. Supercond*., vol. 27, no. 4, June 2017, Art. no. 4003505

[9] G. Vallone, "Mechanical Design Analysis of MQXFB, the 7.2 m long Low-β Quadrupole for the High Luminosity LHC Upgrade", *IEEE Trans. Appl. Supercond*., vol. 28, no. 3, 2018, Art. no. 4003705

[10] H.-G. Brokmeier, W.M. Gan, C. Randau, M. Voeller, J. Rebelo-Kornmeier, M. Hofmann, "Texture analysis at neutron diffractometer STRESS-SPEC", *Nuclear Instruments and Methods in Physics Research A*, vol. 642, pp. 87-92, 2011

[11] C. Randau, H.G. Brokmeier, W.M. Gan, M .Hofmann, M. Voeller, N. Al-hamdanya, G. Seidl, "Improved sample manipulation at the STRESS-SPEC neutron diffractometer using an industrial 6-axis robot for texture and strain analyses", *Nuclear Instruments and Methods in Physics Research A*, vol. 794, pp. 67-74, 2015

[12] K. R. Keller and J. J. Hanak, "Lattice softening in single crystal Nb_3Sn", *Phys. Lett*., vol. 21, no. 3, pp. 263–264, 1966

[13] H. Kiewel, H.J. Bunge, L. Fritsche, *Textures and Microstructures*, vol. 28, pp. 261-271, 1997

[14] N.J. Park, H.J. Bunge, *J. Mater. Sci. Forum*, 157-162, 1994, pp. 1663-1670

[15] W. Voigt, „Lehrbuch der Kristallphysik, Teubner, Berlin, 1910

[16] A. Reuss, „Berechnung der Flieflgrenze von Mischkristallen auf Grund der Plastizittsbedingung fiir Einkristalle", *Z. Angew. Math. Mech*., vol. 9, 1929, 49

[17] R. Hill, "The elastic behaviour of a crystalline aggregate", *Proc. Phys. Soc*., vol. A65, 1952, pp. 349-354.

[18] F. Bertinelli, S. Comel, P. Harlet, G. Peiro, A. Russo, A. Taquet, "Production of Low-Carbon Magnetic Steel for the LHC Superconducting Dipole and Quadrupole Magnets", *IEEE Trans. Appl. Supercond*. vol. 16, no. 2, 2006, pp 1777-1781

[19] F. Bertinelli, F. Fudanoki, T. Komori, G. Peiro, L. Rossi, "Production of Austenitic Steel for the LHC Superconducting Dipole Magnets", *IEEE Trans. Appl. Supercond*., vol. 16, no. 2, 2006, pp 1773-1776

[20] "CEP DISCUP® high-performance copper alloys", product information http://www.cep-freiberg.de/media/pdf/CEP-Product-Information_english.pdf

[21] C. Scheuerlein, B. Fedelich, P. Alknes, G. Arnau, R. Bjoerstad, B. Bordini, "Elastic anisotropy in multifilament Nb_3Sn superconducting wires", *IEEE Trans. Appl. Supercond*., vol. 25, no. 3, 2015, Art. no. 8400605

[22] F. Wolf, F. Lackner, M. Hofmann, C. Scheuerlein, D. Schoerling, D. Tommasini, "Effect of epoxy volume fraction on the stiffness of Nb_3Sn Rutherford cable stacks," *IEEE Trans. Appl. Supercond*., submitted

[23] C. Scheuerlein, U. Stuhr, L. Thilly, "In-situ neutron diffraction under tensile loading of powder-in-tube Cu/Nb_3Sn composite wires: effect of reaction heat treatment on texture, internal stress state and load transfer", *Appl. Phys. Lett*., vol. 91, no. 4, 2007, Art. no. 042503,

[24] "Heat Treating of Aluminum Alloys", ASM Handbook, Volume 4: Heat Treating, pp 841-879, ASM International, 1991

[25] M. Moghaddam, A. Zarei-Hanzaki, M.H. Pishbin, A.H. Shafieizad, V.B. Oliveira, " Characterization of the microstructure, texture and mechanical properties of 7075 aluminum alloy in early stage of severe plastic deformation", *Materials Characterization*, vol. 119, 2016, pp. 137-147

[26] C. Scheuerlein, B. Rehmer, M. Finn, C. Meyer, M. Amez-Droz, F. Meuter, K. Konstantopoulou, F. Lackner, F. Savary, J.-Ph. Tock, "Thermomechanical properties of polymers for use in superconducting magnets", *IEEE Trans. Appl. Supercond*., submitted